

MOL 97527

Agonist binding and desensitization of the mu-opioid receptor is modulated by phosphorylation of the
C-terminal tail domain.

William T Birdsong, Seksiri Arttamangkul, James R Bunzow, John T Williams
Vollum Institute, Oregon Health & Science University, Portland, OR 97239

MOL 97527

Mu-opioid Receptor Agonist Binding and Desensitization

Corresponding Author:

William T Birdsong

Vollum Institute L474

Oregon Health & Science University

3181 SW Sam Jackson Park Rd.

Portland, OR 97239

Ph.: (503) 494-4723

Fax: (503) 494-6972

Email: birdsong@ohsu.edu

Pages: 30

Tables: 0

Figures: 5

References: 35

Abstract: 205

Introduction: 505

Discussion: 1399

Abbreviations: ConA, Concanavalin A; DAMGO, [D-Ala², N-MePhe⁴, Gly-ol]-enkephalin; DermA594, Dermorphin-Alexa594; HEK293, human embryonic kidney 293 cells; IMD, intermediodorsal nucleus of the thalamus; LC, locus coeruleus; MD, mediodorsal nucleus of the thalamus; ME, [Met⁵]-enkephalin; MOPr, mu-opioid receptor.

MOL 97527

Abstract:

Sustained activation of G protein-coupled receptors can lead to a rapid decline in signaling through acute receptor desensitization. In the case of the mu-opioid receptor (MOPr) this desensitization may play a role in the development of analgesic tolerance. It is understood that phosphorylation of MOPr promotes association with β -arrestin proteins, which then facilitates desensitization and receptor internalization. Agonists that induce acute desensitization have been shown to induce a non-canonical high-affinity agonist binding state in MOPr—conferring a persistent memory of prior receptor activation. In the current study, live-cell confocal imaging was used to investigate the role of receptor phosphorylation in agonist binding to MOPr. A phosphorylation cluster in the C-terminal tail of MOPr was identified as a mediator of agonist-induced affinity changes in MOPr. This site is unique from the primary phosphorylation cluster responsible for β -arrestin binding and internalization.

Electrophysiological measurements of receptor function suggest that both phosphorylation clusters may play a parallel role during acute receptor desensitization. Desensitization was unaffected by alanine mutation of either phosphorylation cluster, but was largely eliminated when both clusters were mutated. Overall, this work suggests that there are multiple effects of MOPr phosphorylation that appear to regulate MOPr function, one affecting β -arrestin binding and a second affecting agonist binding.

MOL 97527

Introduction:

The mu-opioid receptor (MOPr) is thought to be regulated by receptor phosphorylation (Williams et al., 2013). This phosphorylation may play an important role in adaptations to long-term opioid use such as the development of tolerance. Canonically, phosphorylation of the C-terminal tail of MOPr leads to recruitment of β -arrestin protein to the receptors, interrupting G protein-mediated signaling and promoting receptor internalization (Gainetdinov et al., 2004). Loss of β -arrestin 2, however, does not abolish desensitization of G-protein signaling suggesting that perhaps other mechanisms exist to induce acute desensitization (Dang et al., 2009; Quillinan et al., 2011; Dang and Christie, 2012). Additionally, there are multiple possible phosphorylation sites in the C-terminal tail of MOPr many of which are not directly involved in β -arrestin recruitment. Thus there are potentially multiple mechanisms by which receptor phosphorylation may influence opioid signaling.

An increase in the binding affinity of MOPr for a fluorescent agonist Dermorphin conjugated to Alexa-594 (DermA594) in response to prior agonist exposure has been described previously (Birdsong et al., 2013). The increase in affinity was primarily the result of a decrease in the rate of DermA594 unbinding from the receptor. Prolonged treatment with high efficacy agonists slowed the rate of DermA594 unbinding more than partial agonist. This phenomenon mimics the agonist dependence of acute receptor desensitization. The increased affinity persisted for tens of minutes after washout of agonist and was insensitive to loss of β -arrestin proteins and G-protein signaling. Thus treatments that induce receptor desensitization also induce a high affinity state of the receptor in a manner that is independent of the classical β -arrestin binding/ receptor internalization pathway.

The aim of the current study was to investigate the mechanism of induction of the slowly dissociating state of MOPr and to determine whether this state plays a role in acute receptor desensitization. The hypothesis was that the high affinity state is the result of phosphorylation of the C-terminal tail resulting

MOL 97527

in desensitization. Of the 11 serine and threonine residues in the C-terminal tail, two serine/threonine clusters (proximal residues between 354-357 and distal residues between 375-379 termed “TSST” and “STANT” after their amino acid sequences, respectively) are differentially phosphorylated by DAMGO over morphine (Lau et al., 2011; Chen et al., 2013). Alanine mutation of the TSST cluster in the proximal C-terminal tail dramatically attenuated the agonist-induced slowing of DermA594 unbinding. This phosphorylation cluster did not reduce β -arrestin binding or receptor internalization while both were blocked after mutation of the STANT cluster (Lau et al., 2011). To determine whether these phosphorylation clusters played a role in acute desensitization, phosphorylation-deficient MOPr mutants were introduced into mouse thalamic neurons and locus coeruleus neurons. Electrophysiological recordings from acute brain slices demonstrated that mutation of both TSST and STANT clusters were required to significantly reduce the amount of agonist-induced receptor desensitization. Mutation of TSST or STANT alone had no effect on acute desensitization. These results suggest that there may be at least two parallel phosphorylation-dependent pathways that reduce the signaling of MOPr: one dependent on STANT phosphorylation/ β -arrestin binding and another, which mediates TSST phosphorylation/ agonist-receptor interactions.

Materials and Methods:

Drugs: Morphine was provided by National Institute on Drug Abuse Neuroscience Center, [Met⁵]-enkephalin (ME), or [D-Ala², N-MePhe⁴, Gly-ol]-enkephalin (DAMGO) and concanavalin A (ConA) were from Sigma Aldrich (St. Louis, MO). Dizocilpine maleate (MK801) was from Abcam (Cambridge, MA). Alexa-488 SDP ester (Life Technologies, Eugene, OR) was conjugated to M1 anti FLAG antibody (Sigma Aldrich) and purified using Bio-Spin 6 Tris columns (Bio-Rad, Hercules, CA).

Cloning and Transfection: HEK293 cells stably expressing wild type, TSST-4A, and STANT-3A and C-terminal 11-alanine murine FLAG-MOPr were a gift from Dr. Mark von Zastrow. Other constructs were

MOL 97527

created by site directed mutagenesis of wild type FLAG-MOPr in the pcDNA3 plasmid (Life Technologies, Eugene, OR). For creation of transiently or stably transfected cells, HEK293 cells were transfected in 6 well plates using Lipofectamine 2000 (Life Technologies) following manufacturer's protocol. Cells were cultured in DMEM +10% Fetal Bovine Serum (+G418, 0.8%, for stable cells, Sigma Aldrich).

Fluorescent Ligand Synthesis: DermA594 was synthesized from Dermorphin analogue (Tyr-D-Ala-Phe-Gly-Tyr-Pro-Lys-Cys-amide) and Alexa Fluor®594 C₅-maleimide (Life Technologies) as described previously (Arttamangkul et al., 2000; Birdsong et al., 2013), purified by HPLC and the molecular mass verified by mass spectrometry (Bioanalytic Shared Resources/ Pharmacokinetic Core, Oregon Health & Science University).

HEK293 Cell Imaging: Cells were plated on poly-lysine coated 12 mm round glass coverslips (Neuvitro, El Monte, CA) and underwent various pharmacological treatments as described. FLAG-MOPr was visualized using an M1 anti-FLAG antibody directly conjugated with Alexa 488 (M1-A488). Drug treatment was performed at 37°C in the presence of Concanavalin A (ConA 600 µg/mL, Sigma Aldrich) to reduce receptor internalization. Coverslips were placed in the imaging chamber where cells were continually perfused with room temperature ACSF solution containing (in mM): 126 NaCl, 2.5KCl, 1.2 MgCl₂, 2.6 CaCl₂, 1.2 NaH₂PO₄, 11 D-glucose, and 21.4 NaHCO₃ (95% O₂/5% CO₂). It was approximately 5 minutes between the time the coverslips were removed from drug treatment in the incubator and when imaging began. This was ample time to ensure that drugs were thoroughly washed from the cells before DermA594 was applied (see supplementary Figure 1). Imaging was performed as previously described (Birdsong et al., 2013). Briefly, cells were imaged using an upright spinning disk confocal microscope. FLAG-MOPr was excited with a 488nm laser while DermA594 was excited by 561nm laser light. Serial images of 488 and 561 nm excitation were acquired with 200 msec. exposures

MOL 97527

every 2.5 seconds. DermA594 was rapidly applied (generally for 90 seconds) and washed using a glass theta tube flowing either control modified ACSF (ACSF without glucose and NaHCO_3 with 15 mM HEPES-sodium salt added, pH 7.4) or modified ACSF containing 100 nM DermA594. Solution exchange time was well under 1 second, much faster than the 2.5-second interval between image frames. The intensity of DermA594 binding (red) was normalized to the intensity of M1-A488 (green) bound to surface FLAG-MOPr to account for changes in focal plane or cell size during image acquisition. This resulted in a red: green ratio (R/G) that was normalized to the peak R/G value measured immediately after washout of DermA594 and plotted as the relative amount of DermA594 remaining.

Animal Experiments: All experiments with mice were conducted in accordance with the National Institutes of Health Guide for the Care and Use of Laboratory Animals following protocols approved by the Institutional Animal Care and Use Committee at Oregon Health & Science University. Both male and female mice were used in approximately equal numbers.

Viral Injection: Viral plasmids were cloned by inserting N-terminal FLAG tagged wild type, TSST-4A, STANT-3A and C-term-11A FLAG-MOPr into pAAV-mCherry-P2A WPRE vector, derived from pACAGW-ChR2-Venus-AAV (Petreanu et al., 2009). The P2A motif allows for cleavage of mCherry from the FLAG-MOPr resulting in soluble mCherry to identify infected neurons and membrane-targeted FLAG-MOPr (Kim et al., 2011). The University of North Carolina Vector Core (Chapel Hill, NC) produced the AAV2-serotype viruses. Four to six-week old male and female MOPr knockout mice (Schuller et al., 1999) were anesthetized by isoflurane and virus was stereotaxically injected 0.45 mm lateral from midline and -1.4 mm from bregma at a depth of 3.8 mm below the top of the skull into the mediodorsal thalamus. After recovering from surgery, animals were returned to their home cages for 2-4 weeks following injection. For injections into the mouse locus coeruleus (LC), injections were

MOL 97527

performed identically except the injection site was 0.9 mm lateral, -4.7 mm from bregma, and a depth of 3.9 mm below the skull

Tissue Preparation: Mice were anesthetized with isoflurane and decapitated. The brain was gently removed into ice-cold ACSF solution + 0.01 mM MK801. Brain was trimmed and mounted into a vibratome chamber (VT 1200S; Leica, Wetzlar, Germany). Coronal brain slices (230 μ m) were prepared and transferred to a warm ACSF solution + MK801 for 30-45 minutes. After recovery, slices were incubated in ACSF at room temperature until used.

Brain Slice Electrophysiology: Slices were continually perfused with warm (33°C), aerated (95% O₂/5% CO₂) ACSF. Virally transduced cells were identified by their soluble mCherry fluorescence. Whole cell recordings were made from MD neurons using an Axopatch 200A amplifier (Molecular Devices, Sunnyvale, CA) at a holding potential of -60 mV. Glass pipettes (1.8-2.8 M Ω) were filled with a potassium gluconate-based intracellular solution containing (in mM): 110 K-gluconate, 10 KCl, 15 NaCl, 1.5 MgCl₂, 10 HEPES-potassium salt, 1 ethylene glycol-bis (2-aminoethyl ether)-N,N,N',N'-tetraacetic acid (EGTA), 2 Mg-ATP, and 0.2 Na-GTP (pH 7.4, 278 mOsm). Series resistance was monitored and maintained below approximately 15 M Ω for inclusion in analysis. Data were digitized and recorded using a PowerLab digitizer and Chart software (AD Instruments, Colorado Springs, CO).

Desensitization Protocol: Slices were perfused with an approximately half maximal concentration of ME (100 nM) and the outward current was measured. After establishing a steady baseline. A saturating concentration of ME (30 μ M) was applied for 5 minutes (thalamus) or 10 minutes (locus coeruleus) to induce acute receptor desensitization. Following the desensitization, ME was washed and the half-maximal ME concentration was reapplied after 5 min. The measurement of “acute decline” was the baseline-subtracted current amplitude in ME (30 μ M) measured at the end of the application as a

MOL 97527

percentage of the initial current amplitude. The initial current amplitude was subtracted from a baseline immediately preceding ME (30 μ M). The current amplitude at the end of the 5- or 10-minute pulse was subtracted relative to the return to baseline following the washout of ME (30 μ M). If the current did not clearly return to baseline between the desensitization pulse and the 5 minute test pulse (as in the STANT-4A and TSST + STANT 7A examples in figure 5B) the current amplitude was subtracted from a baseline following the washout of the 5 minute 100 nM ME test pulse. For “sustained desensitization”, the baseline subtracted current amplitude in response to the ME (100 nM) test pulse five minutes after washout of the desensitizing pulse was reported as a percentage of the baseline subtracted current amplitude of the ME (100 nM) prepulse.

Brain Slice Imaging: For confocal and widefield images, coronal brain slices were used for electrophysiology experiments and fluorescently labeled with Alexafluor-488 hydrazide (10 μ M) via the intracellular patch pipette solution. Slices were fixed in 4% formaldehyde (Ted Pella Inc, Redding, CA) in phosphate buffered saline for 2 hours. Slices were washed with PBS, mounted on glass slides and imaged. Widefield fluorescence images were obtained using an Olympus MUX10 microscope with a QImaging Retiga 2000R camera. Confocal images were obtained on a Zeiss lsm 780 laser scanning confocal microscope using a 20X air objective at the OHSU Advanced Light Microscopy Core Facility. For two-photon imaging of live slice, cells were labeled with M1 anti FLAG antibody conjugated to Alexa 488 and imaged by excitation at 790 nm on a homebuilt two-photon microscope using scan image software as described previously (Pologruto et al., 2003; Arttamangkul et al., 2008).

Data Analysis: Image quantification was performed using FIJI software (Schindelin et al., 2012) and the Time Series Analyzer plugin (J. Balaji, Department of Neurobiology, University of California, Los Angeles). The fluorescent intensities of regions of interest on the plasma membrane were measured and background subtracted as described previously (Birdsong et al., 2013). The intensity of DermA594 was

MOL 97527

then normalized to the M1-A488 intensity to control for focal drift. Statistics and graphing was performed using Origin (OriginLab, Northampton, MA) and Prism 6 (Graphpad Software, La Jolla, CA). One- or two-way ANOVA were used as appropriate and Tukey's multiple comparison tests were used as a post-hoc analysis to determine statistical significance.

Results:

MOPr retained a memory of prior agonist treatment:

Spinning disk confocal microscopy was used to measure the binding and unbinding kinetics of a fluorescent opioid agonist, Dermorphin conjugated to Alexa 594 (DermA594), to FLAG tagged mu opioid receptors (FLAG-MOPr) stably expressed in HEK 293 cells. Binding of DermA594 (100 nM, 90 sec) was measured under naïve conditions or after cells had been incubated for 2 hours with opioid agonists morphine (10 μ M), [Met]⁵enkephalin (ME, 30 μ M), or [D-Ala², N-MePhe⁴, Gly-ol]-enkephalin (DAMGO, 10 μ M). Consistent with previously reported results, incubation with the partial agonist morphine caused a small decrease in the rate of dissociation of DermA594 compared to untreated cells. In contrast to morphine, treatment with the full agonists ME and DAMGO induced a robust slowing in the rate of dissociation of DermA594 (Figure 1A). This effect was not due to the drugs remaining bound to receptors since the average raw ratio of DermA594: M1 A488 (R/G) either increased or remained constant across all treatment conditions (Supplementary Figure 1A, B). It was previously reported that the slowing in unbinding rate following ME treatment reflects an increase in the affinity of DermA594 for MOPr, thus it is likely that DAMGO and perhaps morphine also increase the affinity of MOPr for DermA594. To compare drug treatment conditions, data were normalized to the peak R/G value of each cell and the area under the curve of the fluorescence was calculated during the first three minutes following washout of DermA594 (Figure 1B). All three agonist treatments increased the area under the curve of DermA594 dissociation, DAMGO and ME significantly more than morphine (ANOVA, Tukey's post hoc $p < .001$ for all treatments vs. untreated). The apparent rate of association (k_{app}) during

MOL 97527

the 90-second application of DermA594 was also measured. Despite morphine having a modest effect on the dissociation of DermA594, morphine, ME, and DAMGO all had a significant effect on the apparent association rate (Figure 1C, ANOVA, Tukey's post hoc ** $p < 0.01$, *** $p < 0.001$ for all treatments vs. untreated). Because the unbinding of DermA594 was not well fit by single exponentials under any condition, the k_{app} could not be used to calculate an affinity change following agonist treatment. These results suggest that morphine, DAMGO, and ME pretreatment all affect MOPr ligand-receptor interactions, potentially through several mechanisms.

MOPr phosphorylation modulated agonist binding:

It has been reported that the C-terminal tail of MOPr becomes phosphorylated differently at multiple sites in an agonist and time-dependent manner (Doll et al., 2011; Lau et al., 2011; Chen et al., 2013) (Figure 2A). Specifically, DAMGO leads to robust and widespread receptor phosphorylation while morphine treatment induces less phosphorylation at fewer sites. The differential effect of DAMGO vs. morphine on dissociation rate mirrors their effects on MOPr phosphorylation under similar conditions. It was hypothesized that receptor phosphorylation in response to agonist treatment may modulate the rate of agonist unbinding and agonist affinity. Serines and threonines in two phosphorylation clusters (Figure 2A) were mutated to alanine and the ability of ME to modulate the unbinding rate of DermA594 from these mutant receptors was determined. Mutation of STANT to AAANA (STANT-3A) had little effect on the ability of ME pretreatment to slow down the rate of DermA594 unbinding after 20 minutes of exposure to ME (30 μ M, Figure 2B left, middle). After 2 hrs. of ME treatment, there was a significant decrease in the area under the curve of DermA594 dissociation. However, multiple comparison analysis revealed no significant interaction between the STANT mutation and ME treatment ($p = 0.4227$). In contrast, mutation of TSST to AAAA (TSST-4A) largely attenuated, but did not completely abolish, the ability of ME to modulate MOPr binding kinetics (Figure 2B right, 2C). The effect of TSST mutation was significant after both 20 minutes and 2 hours and there was a strong interaction effect between

MOL 97527

TSST mutation and ME treatment ($p < 0.001$). Thus, it appears that the TSST motif was involved in mediating the change in MOPr/DermaA594 binding kinetics in response to prior agonist exposure, possibly through phosphorylation of these residues, although there was clearly a secondary component that was TSST-independent. It is unclear exactly how the changes in DermaA594 dissociation kinetics affect DermaA594 binding affinity. The apparent rate of association of DermaA594 at concentrations of 30, 100 and 200 nM was measured before and after ME treatment (30 μ M, 2 hrs.) for both the TSST-4A and STANT 3A mutants (Supplementary Figure 2B). For both TSST-4A and STANT-3A there was a significant effect of ME treatment on slowing the rate of association (Untreated vs. ME 2 hrs.: $p < 0.001$). These data were consistent with ME treatment increasing DermaA594 affinity in MOPr lacking either TSST or STANT phosphorylation sites. The results were not consistent enough to determine the K_d with reasonable accuracy or to compare the relative effects of mutation of TSST and STANT on DermaA594 binding affinity.

The time-course of modulation of DermaA594 binding by ME pretreatment was investigated next to determine whether changes in binding affinity were temporally similar to induction of acute desensitization. Both wild type and TSST-4A FLAG-MOPr were treated with ME (30 μ M) for various times from 2 minutes to 2 hours (Figure 2D). ME was washed and DermaA594 (100nM) was applied for 90 sec as done previously. The area under the curve of the normalized DermaA594 fluorescence during agonist unbinding was determined as in figure 1. ME-induced modulation occurred with both a fast (time constant, $\tau=3$ minutes representing 37.5% of the population) and a slow component ($\tau=80$ min., representing 62.5% of the population). Replacement of TSST with alanine (TSST-4A) resulted in a smaller increase in the fluorescence integral that occurred rather quickly and was best fit with τ s of approximately 4 (38%) and 14 minutes (62%). The difference between WT and TSST-4A became increasingly significant with increasing ME incubation times (30 μ M). These results suggest that the remaining TSST-independent modulation was relatively rapid while the TSST-dependent increase in

MOL 97527

agonist affinity occurred relatively more slowly on the order of tens of minutes to hours. Thus these two changes in agonist-induced binding kinetics may be temporally and physically unique. Furthermore, the TSST-dependent change appears to be somewhat slower than typical acute receptor desensitization, which occurs over 5 to 10 minutes.

To determine whether phosphorylation could be responsible for the agonist-induced TSST-mediated change in agonist affinity, glutamate mutations in the TSST cluster were made to mimic receptor phosphorylation. It has been previously reported that S355 and T357 from the TSST sequence are important in mediating MOPr desensitization to DAMGO (Wang 2002). Therefore, TSST was mutated to TESE to mimic receptor phosphorylation. Dissociation of DermA594 under naïve conditions was significantly slowed relative to wildtype (Figure 3A, F, $p < 0.001$). Following ME treatment (30 μ M, 2 hrs.), dissociation of DermA594 further slowed significantly (AUC: TESE untreated; 88.3 \pm 4.5, TESE + ME; 131.6 \pm 3.00 intensity*sec, $p < 0.001$ vs. untreated TESE), suggesting that glutamate substitution partially mimicked but did not fully occlude the effect of ME treatment. This suggested that perhaps another residue in the TSST cluster was becoming phosphorylated. To address this, we substituted glutamates for all residues in the cluster (TSST-4E). When DermA594 was added to this mutant, the rate of unbinding under naïve conditions was further slowed compared to wild type receptor (Figure 3B, $p < 0.001$). Following exposure to ME, the TSST-4E MOPr showed a significant but more moderate additional slowing in the rate of DermA594 unbinding (AUC: TSST-4E untreated; 99.9 \pm 4.3, TSST-4E + ME; 114.7 \pm 4.2 intensity*sec, $p < 0.05$). This moderate slowing resembled the change in DermA594 dissociation in the TSST-4A (Fig 2B right) mutant presumably reflecting a TSST-independent change. This suggests that by crudely mimicking the charge and size of phosphorylated serine and threonine residues, the rate of DermA594 dissociation from MOPr can be slowed and emphasizes that modification of the C-terminal tail of the receptor can propagate to the binding pocket, affecting agonist binding and, perhaps, receptor function. The difference between TESE and TSST-4E

MOL 97527

suggests that presumably either T354 or S356 is phosphorylated in addition to or in place of S355 and/or T357. In agreement with mass spectrometry data suggesting two phosphorylation sites in the TSST cluster at S356 and T357 (Chen et al., 2013), alanine mutation of TSST restricted to S356 and T357 (TSAA) abolished the effect of ME treatment to a similar extent as mutation TSST-4A (Figure 3E).

Since alanine mutation of TSST alone did not completely eliminate the ME-induced slowing in agonist off-rate and STANT mutation had a small but significant effect, the role of phosphorylation in the entire C-terminal tail was investigated. Mutation of both TSST and STANT (TSST&STANT-7A) or alanine mutation of all serine and threonine residues (C-term 11A) (Figure 3 B, C, D) had no additional effect; ME treatment (30 μ M, 2 hrs.) still had a small but significant effect on the rate of DermA594 dissociation as quantified by the area under the curve (TSST + STANT 7A +/- ME, $p < 0.001$, TSAA and C-term 11A +/- ME, $p < 0.001$). Thus, it appears that only the final two residues within the TSST motif are required to induce an agonist-induced change in DermA594 dissociation, likely through receptor phosphorylation. Noticeably, even when all serine and threonine residues in the C-terminus were mutated, a small persistent effect of ME pre-treatment remained.

Morphine-induced modulation of DermA594 binding was less dependent on TSST:

Morphine induced a small change in DermA594 dissociation kinetics (Figure 1). Following mutation of TSST to alanine the effect of ME treatment on DermA594 kinetics appeared similar to morphine treatment in WT MOPr. This raised the possibility that morphine-dependent modulation of DermA594-MOPr binding was independent of TSST phosphorylation. This was investigated by comparing the dissociation rate of DermA594 from WT, TSAA, and C-term 11A MOPr under control conditions, following morphine treatment (10 μ M, 2 hrs.), or ME treatment (30 μ M, 2 hrs.) (Figure 4 A, B, and C respectively). TSAA mutation induced a small but significant decrease in dissociation of DermA594 relative to WT following morphine treatment (Figure 4D, $p < 0.05$). The C-term 11-A was no different

MOL 97527

from WT following morphine treatment, but had a significantly increased AUC of DermA594 dissociation relative to WT MOPr under naïve conditions (Figure 4D, $p < 0.001$). This makes it difficult to determine whether the effect of morphine was smaller in the C-term 11A relative to WT receptors. Interestingly, there was no difference in the ability of ME and morphine to modulate DermA594 dissociation in the C-term 11-A. This suggests that the modulation that remained following deletion of the phosphorylation sites in the C-terminus did not show the same strong agonist bias that was present in the TSST-dependent modulation.

TSST/ STANT plays a role in acute MOPr desensitization:

The previous results suggest a small rapid decrease in dissociation rate that was independent of phosphorylation of the C-terminal tail of MOPr and a slower more dramatic change that was dependent on phosphorylation of the TSST cluster. Furthermore, phosphorylation of the STANT cluster and S375 in particular has been shown to occur rapidly and to mediate receptor internalization (Doll et al., 2011; Lau et al., 2011; Just et al., 2013). Although TSST appears to be phosphorylated somewhat slowly, it is possible that phosphorylation of TSST, STANT, or both TSST and STANT affect acute desensitization of receptor function. To investigate the role of TSST and STANT on MOPr signaling in live neurons, AAV2 viruses encoding WT or mutant FLAG-MOPr and the soluble fluorescent marker mCherry were injected into the mediodorsal (MD) and intermediodorsal thalamus (IMD) of MOPr knockout mice (MOPr-KO). MOPr function was assessed using whole cell voltage clamp recordings in acute brain slices. The MD/ IMD endogenously expresses MOPr and GIRK with little evidence of delta or kappa opioid receptor expression (Mansour et al., 1994; Erbs et al., 2015). In agreement with these observations, when challenged with ME (30 μM), potassium selective outward currents were recorded in wildtype C57Bl6 mice that were absent in MOPr-KO mice. Injection of mCherry-P2A -FLAG-MOPr AAV2 into the MD/IMD resulted in expression of soluble mCherry and membrane-localized FLAG-MOPr. Infected neurons were identified by their mCherry fluorescence (Figure 5A top, middle) and

MOL 97527

whole cell voltage clamp recordings were made. Some slices were live stained with M1-Alexa 488 to determine whether FLAG-MOPr was successfully cleaved from mCherry and trafficked to the plasma membrane. Two photon imaging of M1A488 stained neurons in live brain slice demonstrated that FLAG-MOPr was successfully inserted into the plasma membrane in both the cell body and dendritic regions of MD neurons while mCherry was soluble and filled infected cells (Figure 5A bottom).

To investigate acute desensitization, slices were challenged with a low concentration of ME (100 nM) before and following prolonged perfusion with a saturating concentration of ME (30 μ M, 5 min.). Two measures of desensitization of GIRK currents were made, which may represent separate processes. One measure is the acute decline in the peak current that occurs in the continued presence of the desensitizing concentration of ME (30 μ M). The second measure is a more sustained desensitization of the current evoked by a low concentration of ME (100 nM) 5 minutes after desensitization relative to that evoked before desensitization. Acute decline and sustained desensitization were measured from currents evoked in infected MD cells expressing WT and mutant receptors (see Materials and Methods). Surprisingly, all groups (WT, TSST-4A, STANT-3A, and TSST/STANT-7A alanine mutations) showed a similar acute decline in the ME-evoked current regardless of MOPr phenotype (Figure 4B, C), though there was such large variability within groups that it may have masked any small differences.

Differences between groups emerged only when comparing the sustained component of desensitization measured using ME (100 nM) tested 5 minutes after desensitization. When both TSST and STANT were mutated to alanine, there was a significant decrease in sustained desensitization ($p < 0.05$) and the current evoked after desensitization was not statistically different from that prior to desensitization ($p = 0.096$, one sample t-test) (Figure 4C). Mutation of either motif alone, however, failed to significantly decrease the amount of sustained desensitization. In summary, mutation of both TSST and STANT together was required to significantly attenuate sustained desensitization in neurons in brain slice but it appears that STANT played a more significant role than TSST in this sustained desensitization, as TSST/STANT-7A

MOL 97527

was not significantly different from STANT-3A in any of the measures of desensitization. Additionally, the acute decline of current in the continued presence of agonist did not directly correlate with measures of sustained desensitization suggesting that either these two measures involved different processes or that the acute decline in signaling was a less sensitive measure of receptor function.

To address the problem of variability in the acute decline experiments, similar experiments were carried out using WT or TSST/STANT-7A expressed in LC neurons in MOR knockout animals. Like recordings in the medial thalamus, both WT and TSST + STANT-7A expressed in LC neurons showed an acute decline in response to saturating ME (30 μ M, 10 min, Figure 5D). In the LC, however there was a small but statistically significant reduction in the acute decline found in mutant TSST+STANT receptors (Figure 5E, $p < 0.05$, two-sample t-test). Despite the longer desensitization time in the LC (10 minutes vs. 5 in the thalamus), the sustained desensitization in the TSST/STANT-7A MOPr mutant was significantly decreased relative to the WT MOPr ($p < 0.05$, two-sample t-test) and, on average, sustained desensitization was eliminated (WT: 78 \pm 4%, TSST/STANT-7A: 101 \pm 7 % of pre-desensitized). Thus, in the LC, acute decline was slightly but significantly attenuated by mutation of both the TSST and STANT motifs. The results suggest that sustained desensitization was more sensitive to TSST and/or STANT phosphorylation than measures of acute decline.

Discussion:

The current study builds on a previous observation that activation of MOPr by desensitizing agonists induces a long-lived high affinity state for agonists but not antagonist (Birdsong et al., 2013). A cluster of threonine and serine residues in the proximal C-terminal tail (TSST) beginning at Thr354 was identified as a major mediator of the slowed agonist dissociation. Alanine mutation of this cluster alone did not affect acute desensitization of MOPr signaling in neurons of the MD thalamus. Mutation of both the TSST and STANT clusters significantly reduced sustained desensitization, although in the LC there

MOL 97527

was also a small and significant decrease in acute decline. The results also suggest that phosphorylation of the C-terminal tail of GPCRs acts as an allosteric modulator of ligand binding.

Agonist-dependent TSST phosphorylation in HEK cells has been demonstrated previously by mass spectrometry (Lau et al., 2011; Moulédous et al., 2012; Chen et al., 2013). Truncation and mutation studies have shown conflicting results on the effect of TSST on desensitization and receptor down-regulation (Burd, 1998; Deng et al., 2000; Wang, 2000; El Kouhen et al., 2001). The DermA594 binding data demonstrate that mutations of TSST affect agonist dissociation kinetics. The TSAA mutant had the same effect as TSST-4A and C-term 11A on DermA594 binding kinetics suggesting that the final two residues in the TSST cluster are the relevant phosphorylation sites, in agreement with mass spectrometry data (Chen et al., 2013). The results measuring acute desensitization suggest that mutations of TSST along with STANT are required to have a functional action. It is possible that TSST phosphorylation induces a non-functional high affinity state of MOPr. STANT phosphorylation, on the other hand may lead to receptor internalization, which should reduce functional receptors. Therefore, TSST and STANT may both affect receptor function pathways— STANT phosphorylation decreases the number of surface receptors while the phosphorylation of TSST inactivates receptors. This is consistent with previous studies identifying multiple parallel pathways that can mediate acute desensitization (Dang et al., 2009).

The functional data presented here suggest that TSST played some role in the process of desensitization or recovery from desensitization and induced a slowly dissociating binding state. Although it is not clear if the two are related, it is tempting to speculate that the TSST-phosphorylated state of MOPr is incapable of GIRK signaling. A previous study found a faster rate of GIRK deactivation following acute desensitization compared to naïve cells (Williams, 2014). This result is the opposite of what would be expected if these slowly dissociating TSST-phosphorylated receptors were functional and actively

MOL 97527

signaling to GIRK but would be consistent with TSST phosphorylation stabilizing an uncoupled conformation of the receptor.

The time course of the change in agonist affinity was relatively slow compared with the time course of acute desensitization (minutes vs. tens of minutes), yet mutation of TSST and STANT together affected receptor desensitization. Phosphorylation of residues in the STANT cluster begins rapidly—on the order of seconds (Doll et al., 2011). Arrestin recruitment can occur in 1-2 minutes followed quickly by receptor internalization (Keith et al., 1996; Wolf et al., 1999; Arttamangkul et al., 2008; Lau et al., 2011). TSST phosphorylation has been demonstrated after 10 minutes of DAMGO and morphine treatment, but the relative amount of phosphorylation is unknown (Chen et al., 2013). Although the time course of phosphorylation of TSST is not known, the amount of phosphorylation of TSST is reportedly increased after 20 minutes of exposure to DAMGO and further increased after 3 hours exposure (Lau et al., 2011; von Zartrow personal communication). Consistent with that result, the change in unbinding rate of DermA594 occurred with a biphasic time course on the order of both minutes and hours of ME exposure. While this study focused on the effect of TSST mutation on acute desensitization using a 5-minute desensitization protocol, TSST phosphorylation may play a more significant role in cellular tolerance following hours of agonist exposure.

In all binding experiments reported here, ConA was used to decrease the amount of receptor internalization. Under normal conditions it is likely that many of the high affinity TSST-phosphorylated receptors would be internalized. While receptor desensitization has been a focus of this study, TSST phosphorylation may affect some aspect of receptor trafficking or function secondary to internalization. For example, TSST phosphorylation may regulate recycling of receptors after internalization (Roman-Vendrell et al., 2012). Alternatively, it has recently been shown that the β 2 adrenergic receptor can signal from endosomes to activate transcription and internalized GPCRs appear capable of signaling

MOL 97527

(Tsvetanova and von Zastrow, 2014). Perhaps TSST phosphorylation alters the function of endocytosed FLAG-MOPr, either positively or negatively, to affect cell function at the level of kinase signaling, transcriptional regulation, or receptor recycling and degradation.

Because most opioid drugs are not easily washed from brain slices, many investigations of opioid receptor desensitization study the acute decline in signaling in the continued presence of agonist. Results from electrophysiological recordings demonstrated a clear difference between the acute decline of current in the presence of saturating agonist concentration and the sustained desensitization measured with a lower concentration of agonist following desensitization— in MD acute decline was not affected by TSST and STANT mutation while sustained desensitization was. In the LC acute decline was slightly decreased but still present while sustained desensitization was eliminated. One explanation for this is that sustained desensitization may be a more sensitive assay and thus small changes to desensitization may not be revealed when measuring acute decline (Borgland et al., 2006). This seems unlikely because other studies have found that muscarinic receptor activation of protein kinase C can increase the amount of acute decline (Bailey et al., 2004) in response to ME treatment without affecting sustained desensitization (Arttamangkul et al., 2015). If sustained desensitization were a more sensitive measurement, anything that affected acute decline would be expected to affect sustained desensitization as well. Thus, these two measures may reflect different forms of desensitization, one transient and one more persistent, mediated by multiple pathways. Further complicating direct comparisons, recovery from desensitization is likely an important aspect of sustained desensitization. Rather than initiating the process of desensitization; phosphorylation of TSST and/ or STANT might maintain MOPr in a desensitized state so that mutation of TSST and STANT facilitated rapid recovery from desensitization. Therefore, acute decline and sustained desensitization may be regulated by multiple or different mechanisms and care must be taken in comparing experiments using these different measures of desensitization.

MOL 97527

Modulation of DermA594 binding by ME was largely attenuated by mutation of TSST, yet there was a clear and significant effect of ME treatment even in the C-term 11-A mutant. This suggests that there are at least two mechanisms regulating MOPr-agonist interactions, one through TSST and the other unknown. The dramatic effect of TSST mutation on the ability of ME to slow the rate of DermA594 dissociation is in contrast with the effect on morphine modulation of MOPr-DermA594 binding. The C-term 11-A mutant had only a small effect on morphine-induced modulation of MOPr. This suggests that morphine-dependent modulation may proceed largely through the unknown pathway while ME uses both pathways. Thus, TSST phosphorylation may be strongly biased towards full agonists such as ME, while the unknown portion may demonstrate less bias. This would be consistent with the proposal that morphine and DAMGO can induce MOPr desensitization through different pathways in HEK cells (Johnson et al., 2006; Kelly et al., 2008).

In summary, the results suggest that agonist-mediated phosphorylation of TSST in the C-terminal tail of MOPr induced a long-lived slowly dissociating interaction between MOPr and opioid agonists. While mutation of TSST or STANT alone did not have a significant effect on acute MOPr desensitization, mutation of both TSST and STANT significantly reduced the amount of sustained desensitization following ME treatment. These results suggest an expanded role for phosphorylation in the regulation of MOPr function beyond β -arrestin recruitment and emphasize that the acute decline in signaling appears to be regulated by mechanisms that are distinct from those mediating more sustained desensitization. Finally, while TSST mutation largely attenuated the ME-induced change in DermA594 dissociation, there was still a persistent effect of ME treatment on DermA594 binding that was independent of serine/threonine phosphorylation in the C-terminal tail domain. Thus TSST, STANT and other unknown residues may play additive or complementary roles in the dynamics of opioid receptor signaling

MOL 97527

depending upon the agonist applied, the time course of opioid exposure, and perhaps the system used to measure MOPr signaling.

MOL 97527

Acknowledgments:

We would like to thank Drs. Mark von Zastrow, Elaine Lau, and Michelle Trester-Zedlitz for helpful discussion and providing stable cell lines and plasmid DNA that made these experiments possible and Erica Levitt for helpful feedback during manuscript preparation.

Author Contributions:

Participated in Research Design: Birdsong, Williams, Arttamangkul

Conducted Experiments: Birdsong

Contributed new reagents: Arttamangkul, Bunzow

Performed data analysis: Birdsong

Wrote or contributed to writing of the manuscript: Birdsong, Williams, Arttamangkul, Bunzow

MOL 97527

References

- Arttamangkul S, Alvarez-Maubecin V, Thomas G, Williams JT, and Grandy DK (2000) Binding and internalization of fluorescent opioid peptide conjugates in living cells. *Mol Pharmacol* **58**:1570–1580.
- Arttamangkul S, Birdsong W, and Williams JT (2014) Does PKC activation increase the homologous desensitization of Mu-opioid receptor? *Br J Pharmacol* **172**:583-592.
- Arttamangkul S, Quillinan N, Low MJ, Zastrow M Von, Pintar J, and Williams JT (2008) Differential Activation and Trafficking of Mu-Opioid Receptors in Brain Slices. *Mol Pharmacol* **74**:972–979.
- Bailey CP, Kelly E, and Henderson G (2004) Protein Kinase C Activation Enhances Morphine-Induced Rapid Desensitization of Mu-Opioid Receptors in Mature Rat Locus Ceruleus Neurons. *Mol Pharmacol* **66**:1592–1598.
- Birdsong WT, Arttamangkul S, Clark MJ, Cheng K, Rice KC, Traynor JR, and Williams JT (2013) Increased agonist affinity at the Mu-opioid receptor induced by prolonged agonist exposure. *J Neurosci* **33**:4118–4127.
- Borgland SL, Connor M, Osborne PB, Furness JB, and Christie MJ (2006) Opioid Agonists Have Different Efficacy Profiles for G Protein Activation, Rapid Desensitization, and Endocytosis of Mu-opioid Receptors. *Biochemistry* **278**:18776 –18784.
- Burd AL (1998) Identification of Serine 356 and Serine 363 as the Amino Acids Involved in Etorphine-induced Down-regulation of the Mu-Opioid Receptor. *J Biol Chem* **273**:34488–34495.
- Chen Y-J, Oldfield S, Butcher AJ, Tobin AB, Saxena K, Gurevich V V, Benovic JL, Henderson G, and Kelly E (2013) Identification of phosphorylation sites in the COOH-terminal tail of the μ -opioid receptor. *J Neurochem* **124**:189–199.
- Dang VC, and Christie MJ (2012) Mechanisms of rapid opioid receptor desensitization, resensitization and tolerance in brain neurons. *Br J Pharmacol* **165**:1704–1716.
- Dang VC, Napier I a, and Christie MJ (2009) Two distinct mechanisms mediate acute mu-opioid receptor desensitization in native neurons. *J Neurosci* **29(10)**:3322–3327.
- Deng HB, Yu Y, Pak Y, O’Dowd BF, George SR, Surratt CK, Uhl GR, and Wang JB (2000) Role for the C-Terminus in Agonist-Induced μ Opioid Receptor Phosphorylation and Desensitization. *Biochemistry* **39**:5492–5499.
- Doll C, Konietzko J, Pöll F, Koch T, Höllt V, and Schulz S (2011) Agonist-selective patterns of μ -opioid receptor phosphorylation revealed by phosphosite-specific antibodies. *Br J Pharmacol* **164**:298–307.
- El Kouhen R, Burd AL, Erickson-Herbrandson LJ, Chang CY, Law PY, and Loh HH (2001) Phosphorylation of Ser363, Thr370, and Ser375 residues within the carboxyl tail differentially regulates mu-opioid receptor internalization. *J Biol Chem* **276**:12774–12780.

MOL 97527

- Erbs E, Faget L, Scherrer G, Matifas A, Filliol D, Vonesch J-L, Koch M, Kessler P, Hentsch D, Birling M-C, Koutsourakis M, Vasseur L, Veinante P, Kieffer BL, and Massotte D (2015) A mu-delta opioid receptor brain atlas reveals neuronal co-occurrence in subcortical networks. *Brain Struct Func* **220**:677-702.
- Gainetdinov RR, Premont RT, Bohn LM, Lefkowitz RJ, and Caron MG (2004) Desensitization of G protein-coupled receptors and neuronal functions. *Annu Rev Neurosci* **27**:107-144.
- Johnson EA, Oldfield S, Braksator E, Gonzalez-Cuello A, Couch D, Hall KJ, Mundell SJ, Bailey CP, Kelly E, and Henderson G (2006) Agonist-selective mechanisms of mu-opioid receptor desensitization in human embryonic kidney 293 cells. *Mol Pharmacol* **70**:676-685.
- Just S, Illing S, Trester-Zedlitz M, Lau EK, Kotowski SJ, Miess E, Mann A, Doll C, Trinidad JC, Burlingame AL, von Zastrow M, and Schulz S (2013) Differentiation of opioid drug effects by hierarchical multi-site phosphorylation. *Mol Pharmacol* **83**:633-639.
- Keith DE, Murray SR, Zaki P a, Chu PC, Lissin D V, Kang L, Evans CJ, and von Zastrow M (1996) Morphine activates opioid receptors without causing their rapid internalization. *J Biol Chem* **271**:19021-19024.
- Kelly E, Bailey CP, and Henderson G (2008) Agonist-selective mechanisms of GPCR desensitization. *Br J Pharmacol* **153** SI :S379-388.
- Kim JH, Lee S-R, Li L-H, Park H-J, Park J-H, Lee KY, Kim M-K, Shin BA, and Choi S-Y (2011) High cleavage efficiency of a 2A peptide derived from porcine teschovirus-1 in human cell lines, zebrafish and mice. *PLoS One* **6**:e18556, Public Library of Science.
- Lau EK, Trester-Zedlitz M, Trinidad JC, Kotowski SJ, Krutchinsky AN, Burlingame AL, and von Zastrow M (2011) Quantitative encoding of the effect of a partial agonist on individual opioid receptors by multisite phosphorylation and threshold detection. *Sci Signal* **4**:ra52.
- Mansour A, Fox CA, Burke S, Meng F, Thompson RC, Akil H, and Watson SJ (1994) Mu, delta, and kappa opioid receptor mRNA expression in the rat CNS: an in situ hybridization study. *J Comp Neurol* **350**:412-438.
- Moulédous L, Froment C, Dauvillier S, Burlet-Schiltz O, Zajac J-M, and Mollereau C (2012) GRK2 protein-mediated transphosphorylation contributes to loss of function of μ -opioid receptors induced by neuropeptide FF (NPFF2) receptors. *J Biol Chem* **287**:12736-12749.
- Petreanu L, Mao T, Sternson SM, and Svoboda K (2009) The subcellular organization of neocortical excitatory connections. *Nature* **457**:1142-1145, Macmillan Publishers Limited. All rights reserved.
- Pologruto TA, Sabatini BL, and Svoboda K (2003) ScanImage: flexible software for operating laser scanning microscopes. *Biomed Eng Online* **2**:13.
- Quillinan N, Lau EK, Virk M, von Zastrow M, and Williams JT (2011) Recovery from mu-opioid receptor desensitization after chronic treatment with morphine and methadone. *J Neurosci* **31**:4434-4443.

MOL 97527

Raveh A, Cooper A, Guy-David L, and Reuveny E (2010) Nonenzymatic rapid control of GIRK channel function by a G protein-coupled receptor kinase. *Cell* **143**:750–760.

Roman-Vendrell C, Yu YJ, and Yudowski GA (2012) Fast modulation of μ -opioid receptor (MOR) recycling is mediated by receptor agonists. *J Biol Chem* **287**:14782–14791.

Schindelin J, Arganda-Carreras I, Frise E, Kaynig V, Longair M, Pietzsch T, Preibisch S, Rueden C, Saalfeld S, Schmid B, Tinevez J-Y, White DJ, Hartenstein V, Eliceiri K, Tomancak P, and Cardona A (2012) Fiji: an open-source platform for biological-image analysis. *Nat Methods* **9**:676–682.

Schuller AG, King MA, Zhang J, Bolan E, Pan YX, Morgan DJ, Chang A, Czick ME, Unterwald EM, Pasternak GW, and Pintar JE (1999) Retention of heroin and morphine-6 beta-glucuronide analgesia in a new line of mice lacking exon 1 of MOR-1. *Nat Neurosci* **2**:151–156.

Tsvetanova NG, and von Zastrow M (2014) Spatial encoding of cyclic AMP signaling specificity by GPCR endocytosis. *Nat Chem Biol* **10**:1061-1066.

Wang HL (2000) A cluster of Ser/Thr residues at the C-terminus of μ -opioid receptor is required for G protein-coupled receptor kinase 2-mediated desensitization. *Neuropharmacology* **39**:353–363.

Williams JT (2014) Desensitization of functional μ -opioid receptors increases agonist off-rate. *Mol Pharmacol* **86**:52–61.

Williams JT, Ingram SL, Henderson G, Chavkin C, von Zastrow M, Schulz S, Koch T, Evans CJ, and Christie MJ (2013) Regulation of μ -opioid receptors: desensitization, phosphorylation, internalization, and tolerance. *Pharmacol Rev* **65**:223–254.

Wolf R, Koch T, Schulz S, Klutzny M, Schroder H, Raulf E, Buhling F, and Holtt V (1999) Replacement of Threonine 394 by Alanine Facilitates Internalization and Resensitization of the Rat μ Opioid Receptor. *Mol Pharmacol* **55**:263–268.

MOL 97527

Footnotes: This work was supported by the National Institutes of Health National Institute on Drug Abuse [DA08163] and National Institute of Neurological Disease and Stroke [P30 NS061800].

MOL 97527

Figure Legends:

Figure 1: High efficacy agonist pre-treatment slowed dissociation of fluorescent agonist DermA594: A) HEK293 cells stably expressing FLAG-MOPr were incubated at 37°C with concanavalin A (black, 600 µg/mL) and morphine (blue, 10µM), DAMGO (white, 10µM), or ME (red, 30µM) for two hours. Following incubation, cells were washed and imaged at RT while DermA594 (100nM) was applied for 90 seconds and then rapidly washed. DermA594 fluorescence intensity on the plasma membrane was normalized to the intensity at the end of the 90-second application and single examples are plotted. The area under the curve (AUC) during the first 3 minutes of DermA594 dissociation is shaded in gray for untreated FLAG-MOPr. B) Summarized data plot the AUC of the normalized DermA594 fluorescent signal for the first 3 minutes following washout of DermA594 (n=7-9, avg. +/- s.e.m.). Morphine, DAMGO, and ME treatment all significantly increased the AUC relative to untreated cells. C) The apparent association rate ($k_{(app)}$) was determined under each treatment condition (untreated, morphine (10µM), DAMGO (10µM), or ME (30µM) for 2 hrs.) and is plotted, (n=6-7, avg. +/- s.e.m.) (**, $p < 0.01$; ***, $p < 0.001$ relative to untreated; ###, $p < 0.001$ relative to morphine treatment, one-way ANOVA, Tukey's post hoc)

Figure 2: Phosphorylation motif involved in agonist modulation of MOPr binding affinity. A) The amino acid sequence of the C-terminus of murine MOPr is depicted beginning with phenylalanine 347. Serine and Threonine residues are shown in red. Two phosphorylation clusters "TSST" and "STANT" are underlined. B) Serine and threonine residues were mutated to alanine within the STANT (middle, STANT-3A) and TSST (right, TSST-4A) cluster. Cells were either untreated (black) or treated for 20 minutes (open) or 2 hrs. (red) with ME (30µM). After washing ME, DermA594 (100nM, 90 sec.) was applied and rapidly washed. Dissociation of DermA594 from WT (left), STANT-3A (middle), and TSST-4A (right) FLAG-MOPr was plotted. C) TSST-4A had less DermA594 bound after 3 minutes of washout of DermA594 relative to WT and STANT-3A (n=6-11, avg +/- s.e.m.). D) Time course of

MOL 97527

modulation by ME. WT and TSST-4A FLAG-MOPr were treated with ME (as in fig 2B) for various times from 2- 120 minutes and washed. The area under the normalized curve for the dissociation of DermA594 was plotted relative to ME treatment time (n=7-9, avg. +/- s.e.m.), (*, $P < 0.05$; **, $p < 0.01$; ***, $p < 0.001$ vs. WT, two-way ANOVA, Tukey's post hoc).

Figure 3: Modulation in the C-terminal tail of MOPr is restricted to TSST. HEK293 cells expressing mutant FLAG-MOPr were untreated (open squares) or treated with ME (30 μ M) for 2 hrs. (closed squares) and DermA594 (100 nM, 90 sec) was added and then washed. Dissociation of DermA594 was measured and plotted. Previously shown data with WT FLAG-MOPr were superimposed with light gray (untreated) and light red (ME 2 hrs.) lines. A-B) TSST to TESE (TEST) and TSST to EEEE (TSST-4E) were used to mimic phosphorylation. B-E) TSST to TSAA (TSAA) attenuated the ME-induced modulation of DermA594 binding to approximately the same extent as mutation of TSST + STANT to AAAA + AANA (TSST/STANT-7A) or mutation of all 11 serine and threonine residues in the C-terminal tail to alanines (C-term 11A) (n=4-6, avg. +/- s.e.m.). D) Summarized data plotting AUC for the first 3 minutes of DermA594 dissociation for the mutants that were graphed above. WT MOPr AUC is drawn as light grey line (untreated) and light red line (ME, 2 hrs.) for comparison. Statistics compare mutant vs. WT under the same treatment conditions (either untreated or ME treated) (n=5-15, avg. +/- s.e.m.).

Figure 4: C-terminal mutation had only a modest effect on morphine-induced modulation of binding. HEK 293 cells expressing WT, TSAA, and C-term 11-A MOPr were untreated (A), or treated with morphine (B, 10 μ M, 2 hrs.) or ME (C, 30 μ M, 2 hrs.). The normalized relative amount of DermA594: M1-A488 is plotted immediately following DermA594 exposure (100 nM, 90 sec). D) AUC for the first 3 minutes of DermA594 dissociation is plotted for each condition. (*, $p < 0.05$; ***, $p < 0.001$ vs. WT under same drug treatment condition, two-way ANOVA, Tukey's post hoc) (n=5-15, avg. +/- s.e.m.).

MOL 97527

Figure 5: C-terminal serine and threonine residues are involved in sustained acute desensitization. A) FLAG-MOPr + mCherry AAV2 was injected into the MD thalamus of MOPr KO mice. Coronal brain slices were made and an mCherry expressing cell was filled with Alexa 488. The fixed coronal brain slice was imaged using widefield fluorescence (top) or laser scanning confocal microscopy (middle). Confocal image of an Alexa 488 (green) filled cell also expressing mCherry (red), (merged in yellow) among other AAV2 infected cells from the brain slice pictured above. Scale: 40 μm . Bottom: two-photon images of a live brain slice showing neurons in MD thalamus expressing mCherry (left) and stained with M1-Alexa 488 anti-FLAG antibody (middle) and overlaid in the merged image (right). Scale: 10 μm . B) Exemplary whole-cell electrophysiological recordings from wildtype and mutant FLAG-MOPr expressing cells. Slices were treated with an approximately EC₅₀ concentration of ME (100 nM). Cells were desensitized with ME (30 μM , 5 minutes) and then retested with EC₅₀ ME 5 minutes later. C) Summary data show the percentage of the current remaining following desensitization in the continued presence of ME 30 μM (Acute Decline) and the percent amplitude of the EC₅₀ ME measured 5 minutes after desensitization relative to the current evoked prior to desensitization (EC₅₀ 5 minutes) in individual cells (open circles) and as an average (avg. +/- s.e.m. n= 9-10 slices, 6-10 animals). D) FLAG-MOPr + mCherry AAV2 was injected into LC of MOPr KO mice and representative whole-cell voltage clamp recordings are shown for WT or TSST/ STANT-7A MOPr. A sub-saturating concentration of ME (100 nM) was applied before and following a 10-minute super-saturating concentration of ME (30 μM , 10 minutes) to induce acute desensitization. E) Acute decline in the continued presence of agonist and sustained desensitization (EC₅₀ 5 minutes) were measured as described above. Average and individual measurements (cyan open circles) are plotted (avg +/- s.e.m. n= 6-7 slices, 4-5 animals.) *, p<.05 compared to WT, One-way ANOVA, Tukey's post hoc.

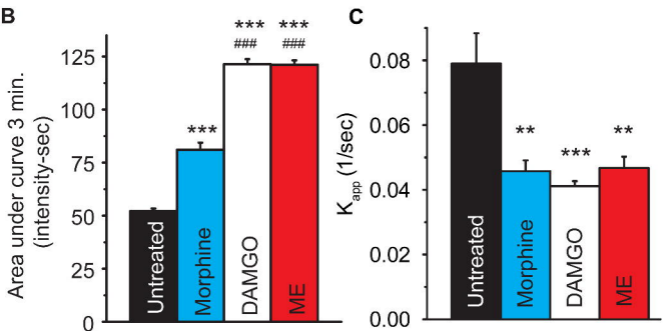
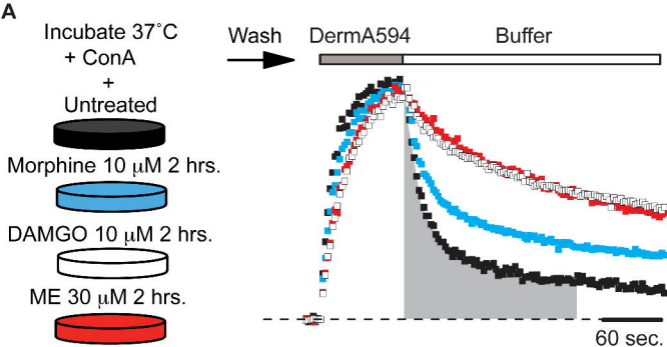


Figure 1

MOR C-Terminal tail sequence:

₋₃₄₇FREFCIP₃₅₄TSSTIEQQN₃₆₃SARIRQN₃₇₀TREHP₃₇₅STANTIVDR₃₈₃TNEQLENLEAE₃₉₄TAPLP

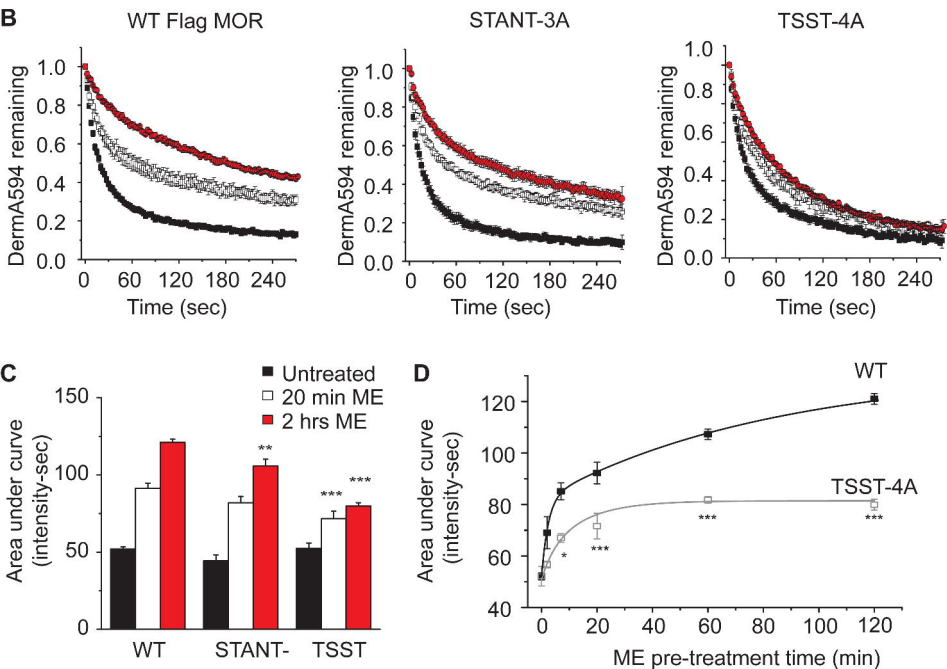


Figure 2

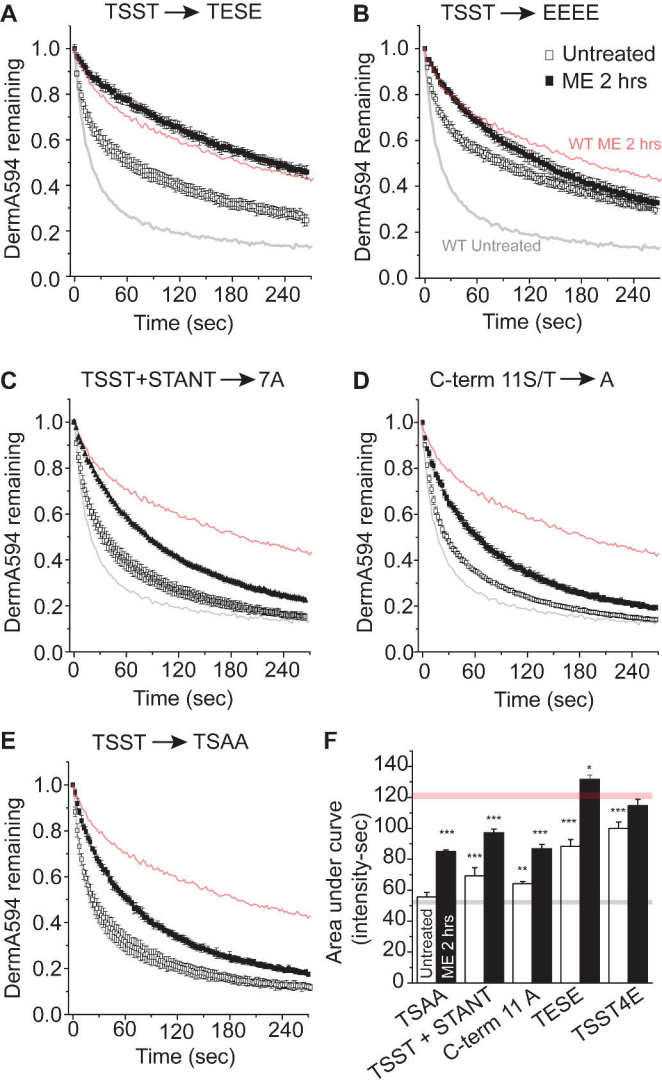


Figure 3

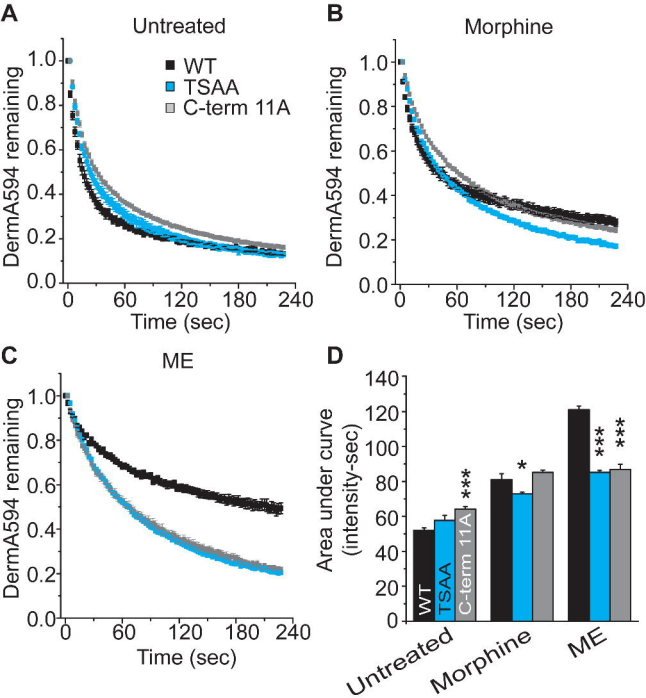


Figure 4

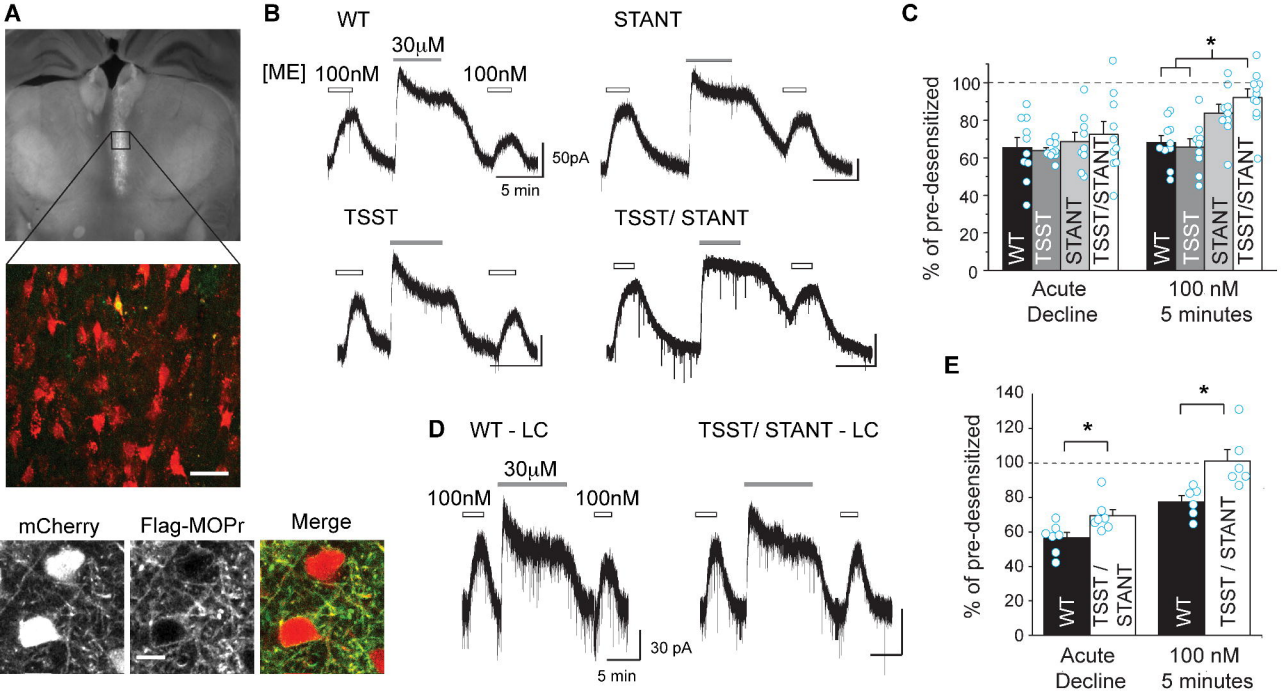


Figure 5